SUPPORTING INFORMATION

Supramolecularly interactive terminal side chains enhance robustness of hydrogel materials

Yuka Wakayama,[a] Taku Sakurai,[a] Takahiro Okabe,[a,b] and Takuma Kureha*[a,b]

[a]Graduate School of Science and Technology, Hirosaki University, 3 Bunkyo-cho, Hirosaki, Aomori 036-8561, Japan

[b]Institute of Global Well-being Science, Hirosaki University, 5 Zaifu-cho, Hirosaki, Aomori 036-8562, Japan

E-mail: t-kureha@hirosaki-u.ac.jp

Table of Contents

1 Experimental section

1.1 Materials……S2
1.2 Synthesis of gels……S2
1.3 Gel-drop rebound tests……S2
1.4 Compression tests……S3
1.5 Swelling ratio measurement and analysis……S4
1.6 Dynamic viscoelasticity measurements……S5
1.7 Gel transmittance measurements……S5
1.8 High-speed gel-drop impact imaging……S6

2 Supplementary results and figures

2.1 Figure S1. Replicate stress–strain curves under uniaxial compression……S7
2.2 Figure S2. Batch-to-batch reproducibility of compressive properties……S8
2.3 Figure S3. Photographs of pOEGh(M) specimen before/after compression……S9
2.4 Figure S4. Cyclic consecutive loading–unloading compression tests……S10
2.5 Figure S5. Stress-relaxation tests and relaxation time……S11
2.6 Figure S6. Replicate temperature-dependent rheology……S12
2.7 Figure S7. Temperature-dependent dynamic viscoelasticity during cooling and optical transmittance……S13
2.8 Figure S8. Effect of crosslinker content (EGD) on pOEGm(M) gels……S14
2.9 Figure S9. Normalized height from high-speed gel-drop impact imaging……S15
2.10 Figure S10. Compression tests for pAAm-based copolymer gels……S16
2.11 Caption of Movie S1……S17

3 Supplementary references

1 Experimental Section

1.1 Materials

Oligo(ethylene glycol) methyl ether methacrylate (OEGm, average M_n = 300 g/mol, n = 4 or 5; M_n = 500 g/mol, n = 8 or 9), Oligo(ethylene glycol) methacrylate (OEGh, average M_n = 360 g/mol, n = 6 or 7; M_n = 500 g/mol, n = 8 or 9), and ethylene glycol dimethacrylate (EGD, 98%), were purchased from Sigma-Aldrich. Ammonium peroxodisulfate (APS, 95%), *N,N,N′,N′*-tetramethyl ethylenediamine (TEMED, 99%), acrylamide (AAm, 98%), and *N,N′*-methylenebis acrylamide (BIS, 99%) were purchased from Wako Pure Chemical Industries. Acid Red 18 and Acid Blue 92 were purchased from Tokyo Chemical Industry Co., Ltd. All reagents were used as received.

1.2 Synthesis of gels

A series of pOEGm-based gels, pOEGh-based gels, pAAm gels, and copolymer gels were prepared by free-radical (co)polymerization in water. The monomers and crosslinkers were dissolved in deionized water at the desired concentrations. The pre-gel solutions were stirred and degassed under argon. To investigate the effect of crosslinker content on the mechanical properties, the amount of EGD was varied from 1 to 50 mol.% while the total monomer concentration was fixed at 1000 mM. Polymerization was initiated by adding APS (2 mM) and TEMED (32 mM). The resulting solutions were transferred to appropriate containers based on subsequent measurements and maintained for 24 h to form gels. All polymerizations were carried out at 25 °C. It should be noted that pAAm gels were not formed when EGD was used as the crosslinker, and thus, EGD was replaced with BIS for the preparation of pAAm gels.

1.3 Gel-drop rebound tests

Spherical gel specimens were prepared by casting the pre-gel solutions into a spherical capsule mold (45 mm in diameter) and allowing them to polymerize overnight. To enhance the visibility of the falling gels, Acid Red 18 was added to the pre-gel solution for the pOEGm gels at 0.01 mM, while Acid Blue 92 was added to the pre-gel solution for the pOEGh gels at 0.01 mM. Before testing, the gel surface was lightly moistened with distilled water. The gel specimens were then dropped from a height of approximately 0.5 m, and the rebound behavior was recorded by video.

1.4 Compression tests

The compressive mechanical properties of the tested gels were measured using a mechanical testing system (STB1225S, A&D Co., Ltd.) in an unconfined compression mode between two impermeable parallel plates. Before commencing each test, a preload of 0.03 N was applied to ensure complete contact between the sample surface and the plates. For standard compression measurements, cylindrical specimens were compressed at a crosshead speed of 10 mm/min using a 2.5 kN load cell up to a maximum strain of 60% of the original height. For the pAAm-based copolymer gels, the crosshead speed was reduced to 1 mm/min. The engineering stress was calculated by dividing the recorded force by the initial cross-sectional area. The engineering compressive strain was defined as the change in height relative to the original height of the freestanding specimen. The initial compressive modulus (G) was determined as the slope of the stress–strain curve in the strain range of 10–15%. The fracture stress (σ_F) is defined as the maximum stress immediately prior to macroscopic fracture when fracture occurs. If a specimen does not fracture up to the strain limit of our protocol, σ_F is reported as the stress at 60% strain. Reported values represent the average of three specimens prepared from the same batch, and the standard deviation is shown as error bars. To address batch-to-batch reproducibility, the compression tests were additionally performed using three independently prepared batches of the representative formulation, pOEGh(M) (total monomer concentration: 1000 mM; crosslinker: 1 mol.% EGD). The stress-strain curves were highly similar across batches, and the extracted G as well as σ_F were in good agreement with the averages obtained from the within-batch replicates (Figure S2). These results therefore support the reproducibility of the key compressive mechanical metrics reported in this study.

Cyclic consecutive loading–unloading tests were performed in triplicate (n = 3) on independent specimens for 10 cycles without a waiting time, at a crosshead speed of 1 mm min^{-1}, with the maximum strain set to 5% or 15%. The dissipated energy (E_d) was calculated from the area enclosed by the loading–unloading hysteresis loop at each cycle. The compression energy (kJ/m^3) was defined as the area under the loading curve, and the relaxation energy (kJ/m^3) as the area under the unloading curve. The dissipation energy loss per cycle (kJ/m^3) was obtained as the hysteresis-loop area. The dissipation ratio (%) was calculated as (dissipation energy)/(compression energy) × 100. Reported E_d values

represent the average of three independent measurements.

Compression stress-relaxation tests were performed on OEGm(M) and OEGh(M) gels (total monomer concentration: 1000 mM; crosslinker: EGD 1 mol%). Stress-relaxation experiments were conducted using three independent specimens ($n = 3$). Disk-shaped specimens (20 mm diameter, 3 mm thickness) were tested in unconfined compression using a mechanical testing system equipped with a 2.5 kN load cell. The samples were compressed at a crosshead speed of 1 mm/min to the target strains of 5% or 15%, and the strain was then held constant for 1 h while the stress was recorded over time, following a standard stress-relaxation protocol under constant strain. For data presentation, the time axis was shifted such that the moment when the target strain was reached (i.e., the maximum stress immediately after loading) corresponded to $t = 1$ s. The stress was normalized by the maximum stress at the onset of the hold (σ_0), yielding a normalized stress, σ/σ_0. The relaxation time (τ) was defined as the time required for the normalized stress to decrease to 0.9 (i.e., $\sigma/\sigma_0 = 0.9$). Reported τ values represent the average of three independent measurements.

1.5 Swelling ratio measurement and analysis

Swelling tests were conducted to determine the number density of effective elastic chains in the gel network (ν_e). Gel sheets with a thickness of 2 mm were prepared and punched into circular specimens (diameter: 14 mm), yielding three specimens for each composition. To remove residual reagents and to equilibrate the gels, the specimens were immersed in deionized water and allowed to stand for 1 day. The weight of each equilibrium-swollen gel (W_e) was then measured to determine the swelling degree. Before weighing, excess surface water was carefully removed by gently wiping the gel surface. To estimate the crosslink density from the swelling degree, the Flory–Rehner equation for affine polymer networks was applied:[1,2]

$$\nu_e = \frac{\left[\ln\left(1 - \varphi_e\right) + \varphi_e + \chi \varphi_e^{\,2}\right]}{V_1\left[\frac{1}{2}\left(\frac{\varphi_e}{\varphi_0}\right) - \left(\frac{\varphi_e}{\varphi_0}\right)^{1/3}\right]} \quad (1)$$

where ν_e is the number density of effective elastic chains, φ_e is the polymer volume fraction at swelling equilibrium, χ is the Flory–Huggins interaction parameter, V_1 is the molar volume of the solvent (water), φ_0 is the volume fraction of dried state, and φ_e/φ_0

corresponds to the swelling degree. According to Flory–Huggins theory, φ_e was determined by assuming that the polymer volume remains unchanged upon swelling:

$$\varphi_e = \frac{[(W_d / d_m)\times 0.99 + (W_d / d_c) \times 0.01]}{[(W_d / d_m)\times 0.99 + (W_d / d_c) \times 0.01] + [W_e - W_d]} \quad (2)$$

where W_d and W_e are the masses (grams) of dried gel and equilibrium-swollen gel, respectively, and d_m and d_c are the specific gravities (g/cm^3) of the monomer and crosslinker. For the calculation of v_e, W_e was taken as the average of three specimens for each composition. The interaction parameter χ was set to 0.48 based on literature values reported for pOEG-based gels.[3]

1.6 Dynamic viscoelasticity measurements

Dynamic viscoelasticity measurements were performed using a rotational rheometer (MCR 302e, Anton Paar) equipped with a concentric cylinder geometry (CC27). The initiator solution was added to the pre-gel solution while avoiding air incorporation, and the mixture was homogenized by pipetting. The reaction mixture was immediately transferred into the measuring cup pre-installed in the rheometer. The CC27 geometry was fully immersed in the mixture, which was then allowed to polymerize at 25 °C for 12 h. The resulting hydrogel was thus formed in situ and remained integrated with the measuring geometry during the measurements. Oscillatory shear measurements were conducted at a strain amplitude of γ = 1% (within the linear viscoelastic regime). The angular-frequency dependence (0.1–100 rad/s) of the storage modulus (G'), loss modulus (G''), and loss tangent (tan δ) was measured at 25 °C and shown as representative measurements. For temperature-dependent measurements, the sample temperature was increased or decreased within the range of 25–80 °C to the target temperature, held for 30 min for equilibration, and then the frequency sweep was recorded at each temperature. Temperature-dependent measurements were performed in triplicate (n = 3) using independently prepared samples. The temperature-dependent rheology data shown in the main text are representative.

1.7 Gel transmittance measurements

The optical transmittance of the gels was measured at a wavelength of 800 nm using a UV–Vis spectrophotometer (UV-1800, SHIMADZU) equipped with a constant-

temperature water bath (NCB-1220, EYELA). The sample temperature was monitored directly using a thermometer (TM-300, AS ONE), and the system was allowed to equilibrate for 10 min at each temperature prior to measurement. For sample preparation, the pre-gel solution was transferred into a quartz cuvette, and the initiator solution was added to initiate polymerization. After allowing the mixture to polymerize for 24 h, the transmittance of the resulting gel (formed in the cuvette) was measured as a function of temperature.

1.8 High-speed gel-drop impact imaging

Spherical gel specimens were prepared by casting the pre-gel solutions into a spherical capsule mold (30 mm in diameter) and allowing them to polymerize overnight. High-speed gel-drop impact imaging was performed using an experimental setup adapted from a previously reported high-speed drop-impact system.[4] Gel specimens were released from a prescribed height (200 mm) and impacted a flat, rigid substrate (material: sapphire). The impact event was recorded from the side using a high-speed camera (model: FASTCAM SA-Z, Photron) at a frame rate of 30,000 fps, with a spatial resolution of 115 μm/pixel. The time origin was defined as the instant of first contact between the gel specimen and the substrate (t = 0 ms). The specimen height at t = 0 ms was defined as H_0, and the instantaneous specimen height during impact was defined as $H_{(t)}$. The deformation was quantified by the normalized height ($H_{\mathrm{nor}} = H_{(t)}/H_0$) extracted from the high-speed image sequences. Each experiment was repeated at least three times, and representative frame sequences are shown in Fig. 4d–f.

2 Supplementary results and figures

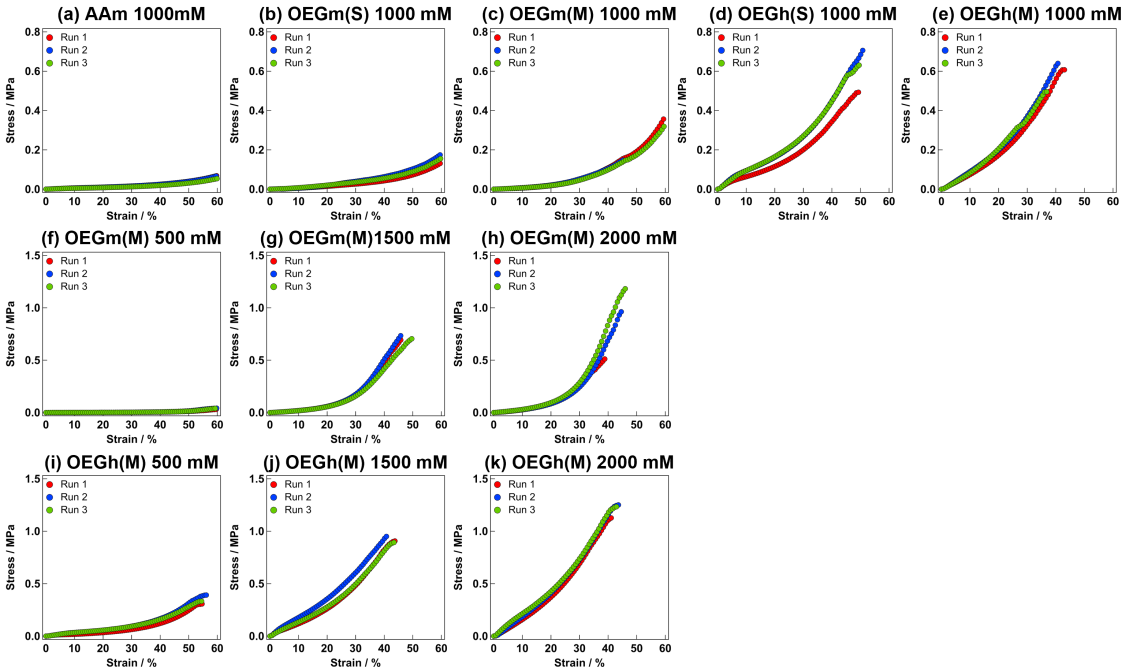

Figure S1. Replicate stress–strain curves under uniaxial compression for the gels investigated in this study (n = 3 for each condition). (a) pAAm, (b) pOEGm(S), (c) pOEGm(M), (d) pOEGh(S), and (e) pOEGh(M) gels, where the total monomer concentration was fixed at 1000 mM. (f–h) pOEGm(M) gels prepared at total monomer concentrations of 500, 1500, and 2000 mM, respectively. (i–k) pOEGh(M) gels prepared at total monomer concentrations of 500, 1500, and 2000 mM, respectively.

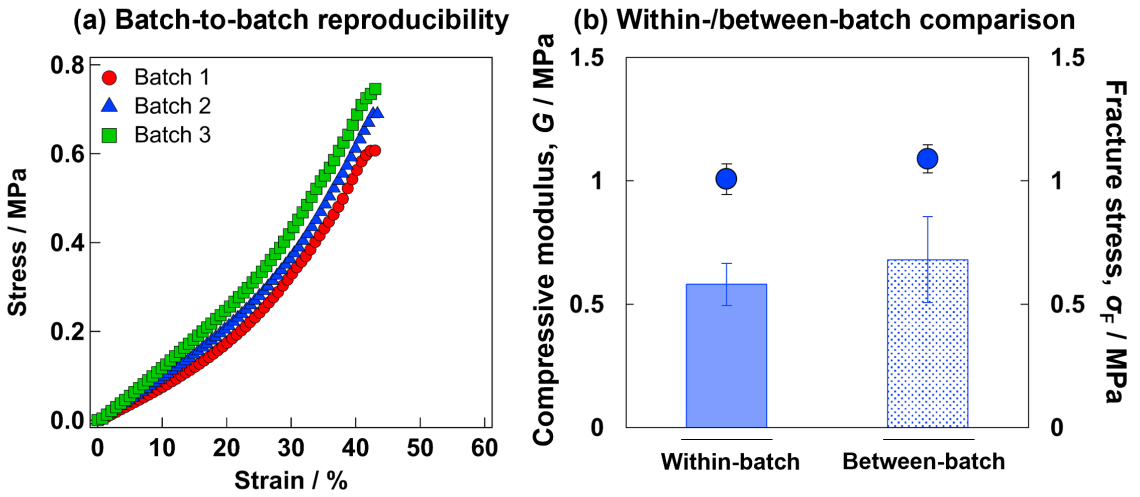

Figure S2. Batch-to-batch reproducibility of compressive mechanical properties for pOEGh(M) gels (total monomer concentration: 1000 mM; crosslinker: 1 mol.% EGD). (a) Representative stress–strain curves for three independently synthesized batches. (b) Comparison of the initial compressive modulus (*G*, circles; left axis) and fracture stress ($\sigma_{F,}$ bars; right axis) between within-batch replicates (three specimens prepared from the same batch; $n = 3$) and independently synthesized batches (between-batch; $n = 3$). Error bars represent the standard deviation.

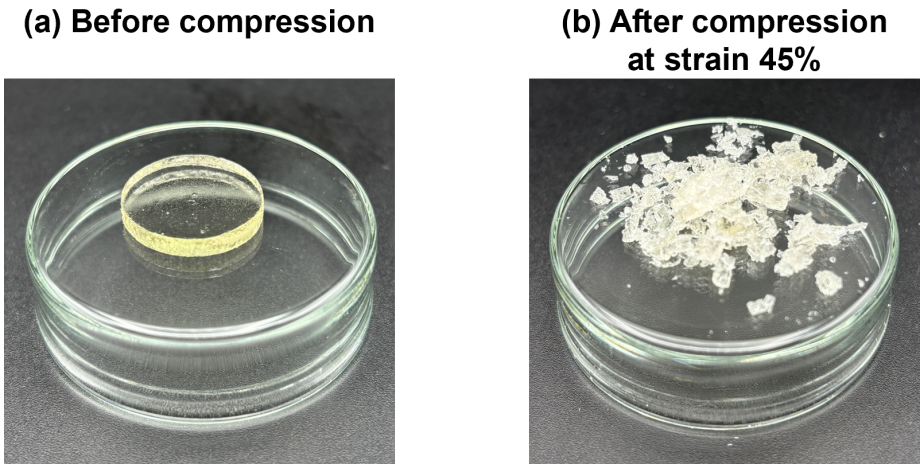

Figure S3. Representative photographs of a pOEGh(M) specimen before and after compression. (a) Gel specimen before compression. (b) Fragmented specimen after compression to 45% strain. This rupture/crack propagation is consistent with the stress drop observed at ~40–50% strain in Fig. 2a.

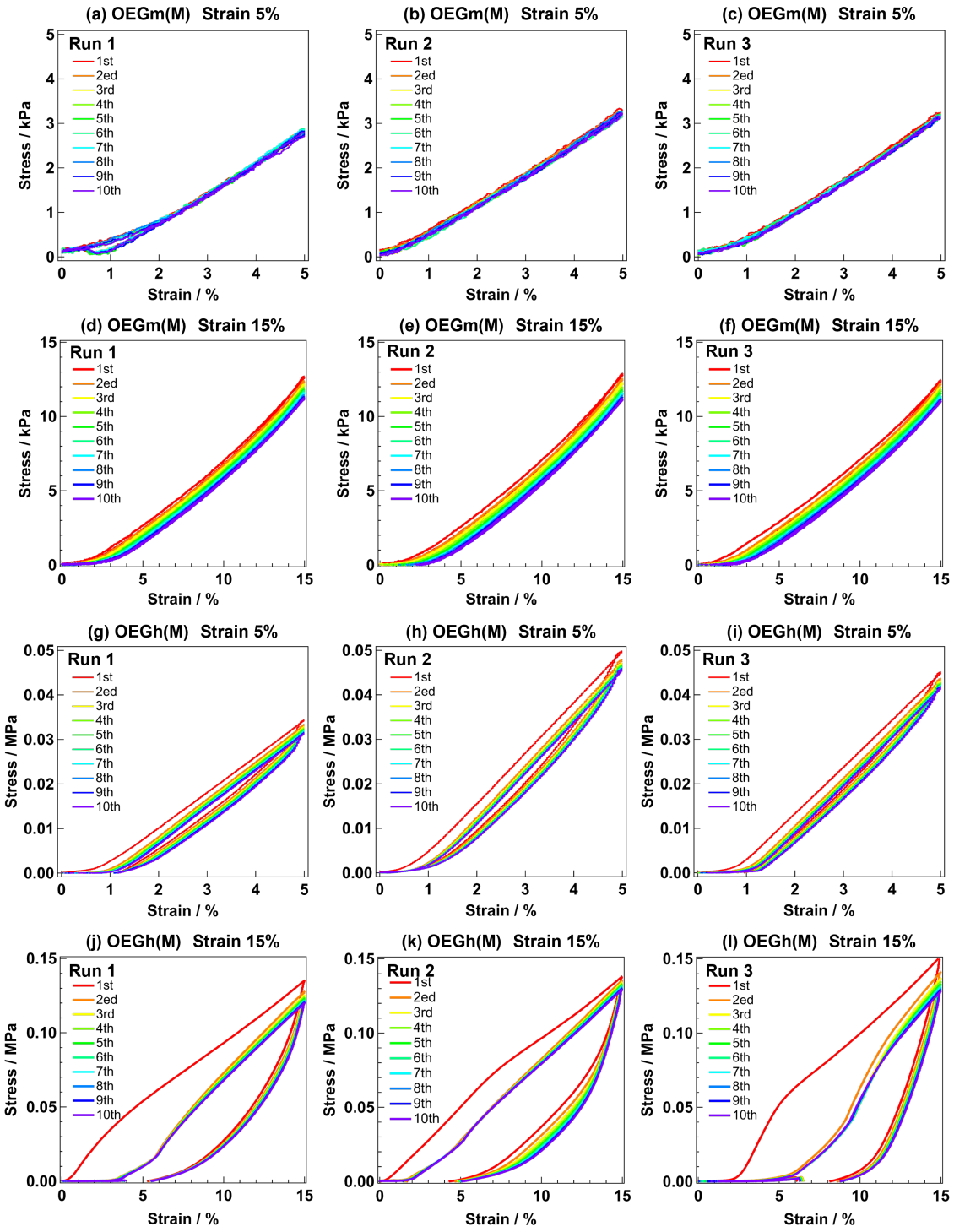

Figure S4. Replicate cyclic loading–unloading behavior under uniaxial compression (n = 3 independent specimens) for pOEGm(M) and pOEGh(M) gels. Compressive stress–strain curves over 10 consecutive cycles at maximum strains of 5% (a–c: pOEGm(M); g–i: pOEGh(M)) and 15% (d–f: pOEGm(M); j–l: pOEGh(M)).

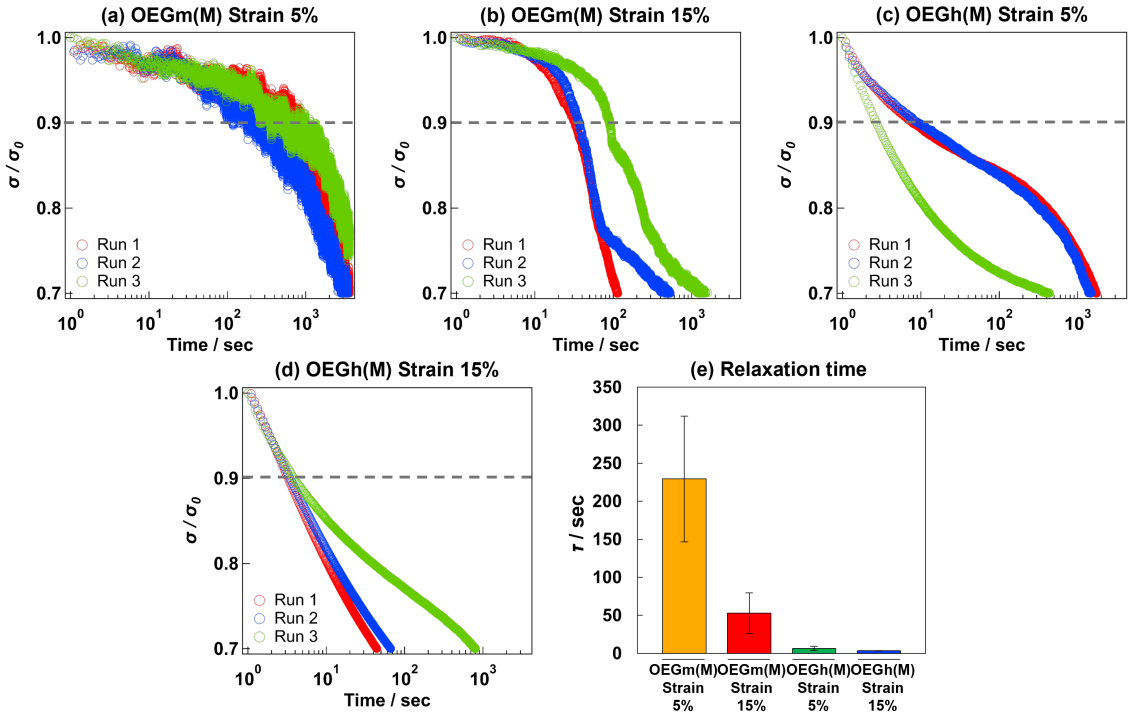

Figure S5. Replicate compressive stress-relaxation behavior (n = 3 independent specimens) for pOEGm(M) and pOEGh(M) gels at 5% and 15% strain. Normalized stress (σ/σ0) as a function of time for pOEGm(M) at (a) 5% and (b) 15% strain, and for pOEGh(M) at (c) 5% and (d) 15% strain. The dashed line indicates $\sigma/\sigma_0 = 0.9$, used to define the relaxation time, τ. (e) The relaxation time, τ, for pOEGm(M) and pOEGh(M) at 5% and 15% strain.

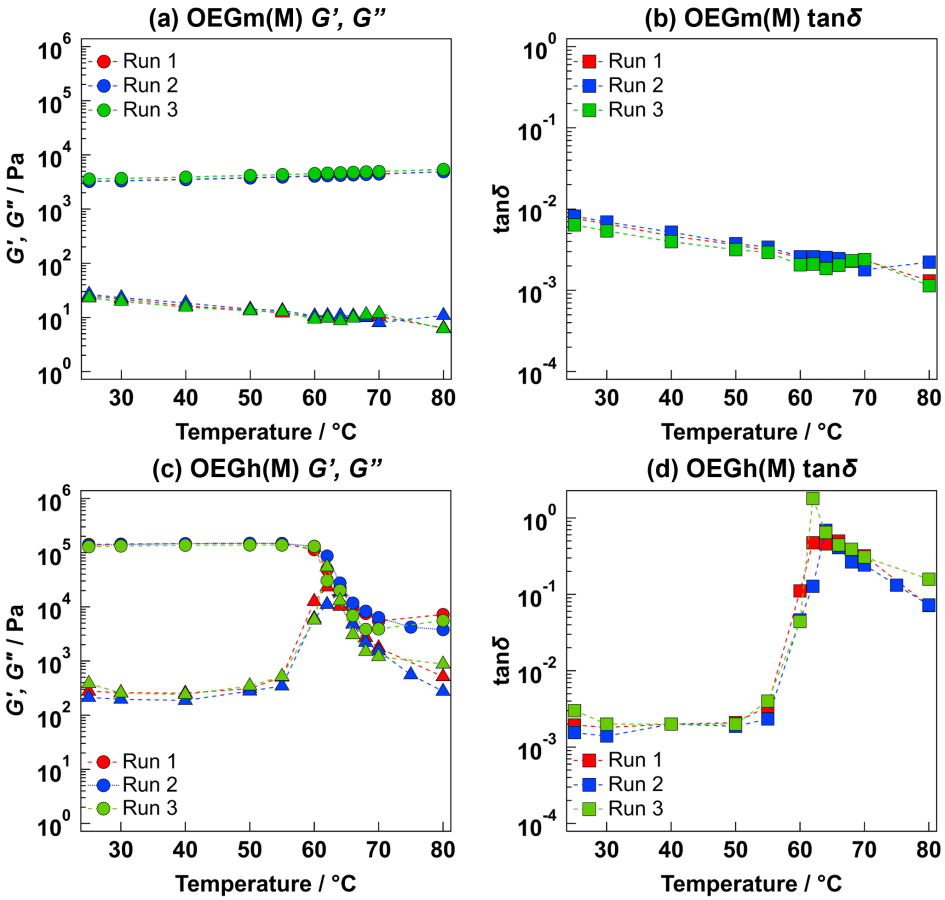

Figure S6. Replicate temperature-dependent dynamic viscoelasticity measurements (n = 3) for pOEGm(M) and pOEGh(M) gels. Temperature dependence of the storage and loss moduli (G'; circles and G''; triangles) for (a) pOEGm(M) and (c) pOEGh(M), and the corresponding loss tangent (tan δ) for (b) pOEGm(M) and (d) pOEGh(M) gels.

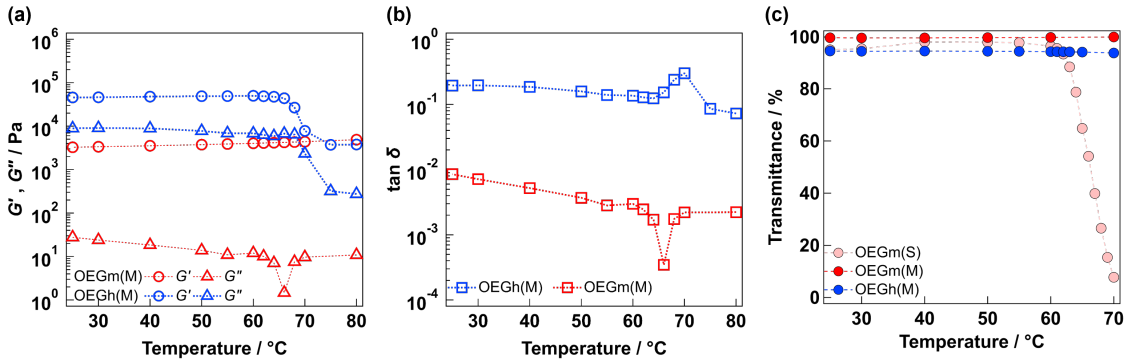

Figure S7. Temperature-dependent dynamic viscoelasticity of pOEGm(M) and pOEGh(M) gels measured under oscillatory shear during cooling: (a) storage and loss moduli (G' and G'') and (b) loss tangent (tan δ) as a function of temperature. (c) Temperature-dependent optical transmittance of each gel measured at wavelength of 800 nm. Transmittance remained essentially unchanged for pOEGh(M) and pOEGm(M) over the temperature range relevant to Fig. 3e,f, whereas pOEGm(S) gels exhibited a marked decrease near its volume phase transition temperature (~ 63 °C).[5]

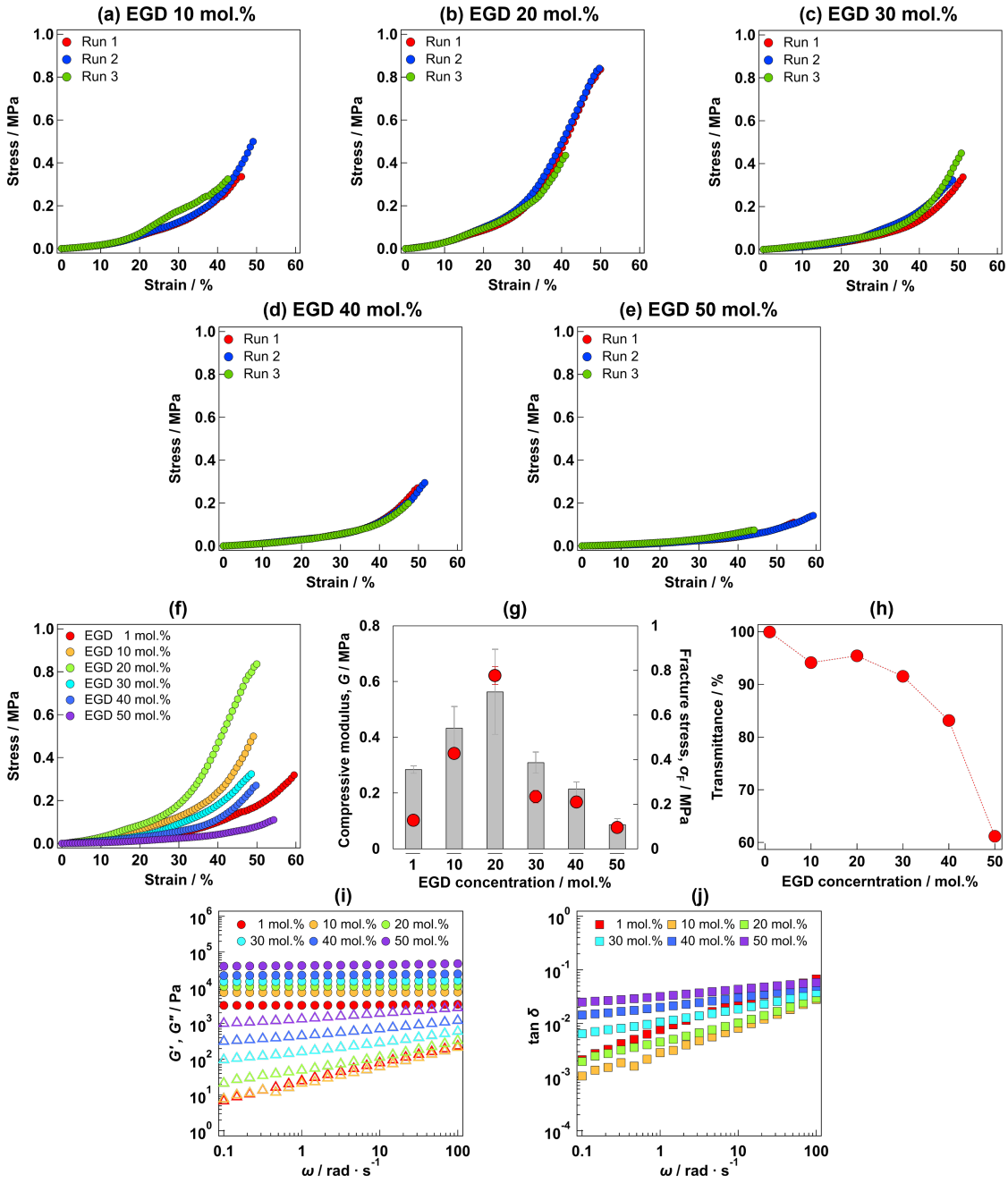

Figure S8. Effect of crosslinker content (EGD) on the mechanical and rheological properties of pOEGm(M) gels: (a–e) replicate compressive stress–strain curves for gels prepared with different EGD contents (n = 3); (f) representative stress–strain curves; (g) summary of the initial compressive modulus (G, symbols; left axis) and fracture stress (σ_F, bars; right axis) as a function of EGD content; (h) optical transmittance of the gels as a function of EGD content at wavelength of 800 nm; (i) angular-frequency dependence of the storage and loss moduli (G' and G'') and (j) the loss tangent (tan δ) for pOEGm(M) gels with different EGD contents.

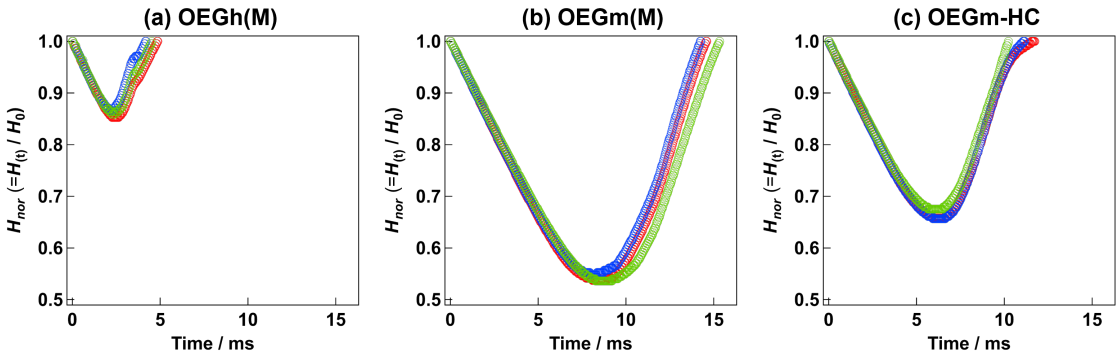

Figure S9. Time evolution of the normalized height, H_{nor} (= $H_{(t)}/H_0$), extracted from high-speed gel-drop impact imaging for (a) pOEGh(M), (b) pOEGm(M), and (c) pOEGm-HC gels (three independent trials for each condition).

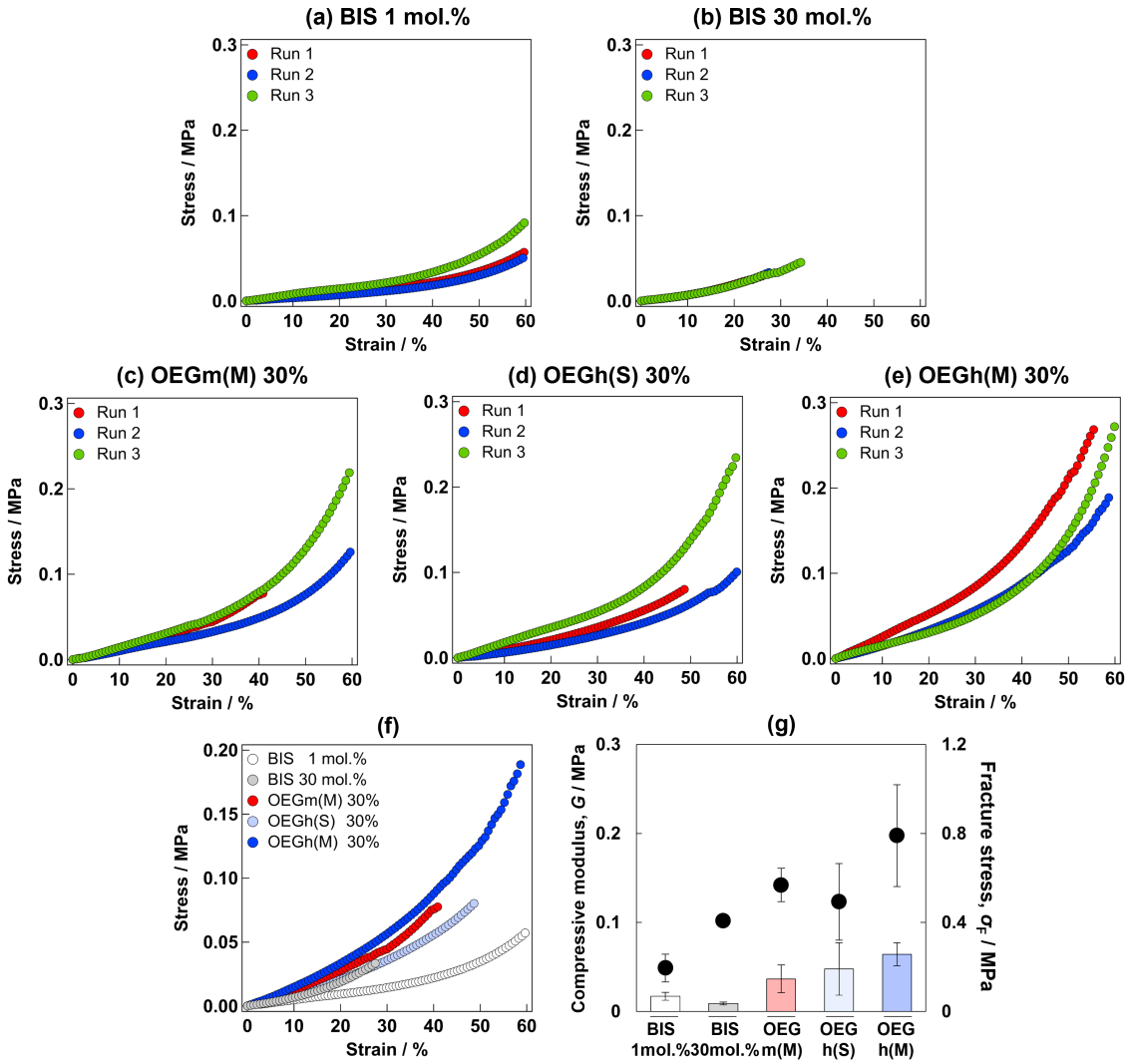

Figure S10. (a–e) Replicate stress–strain curves (n = 3 for each condition) for gels prepared by copolymerizing acrylamide (AAm) with BIS (as a crosslinker) and/or additional comonomers: (a,b) pAAm gels with different BIS contents; (c–e) pAAm-based copolymer gels containing OEG-type comonomers (30 mol.%). (f) Representative stress–strain curves for comparison. (g) Summary of the initial compressive modulus (G, symbols; left axis) and fracture stress (σ_F, bars; right axis).

Movie S1. High-speed gel-drop impact imaging of pOEGh(M), pOEGm(M) and pOEGm-HC gels.

3 Supplementary references

1. P. J. Flory, Principles of Polymer Chemistry, Cornell University Press, Ithaca, 1953
2. N. R. Richbourg and N. A. Peppas, *Prog. Polym. Sci*., 2020, **105**, 101243
3. T. Kureha, T. Hirayama and T. Nishi, *Polym. J.*, 2024, **56**, 1017–1029
4. T. Okabe, K. Shirai, T. Okawa, J. Okajima and M. Shirota, *J. Fluid Sci. Technol.*, 2022, **17**, JFST0009
5. T. Kureha, K. Hayashi, M. Ohira, X. Li and M. Shibayama, *Macromolecules*, 2018, **51**, 8932–8939